

Technetium Complexation with Multidentate Carboxylate-Containing Ligands: Trends in Redox and Solubility Phenomena

Nicole A. DiBlasi,* Kathy Dardenne, Tim Prüssmann, Sarah Duckworth, Marcus Altmaier, and Xavier Gaona*

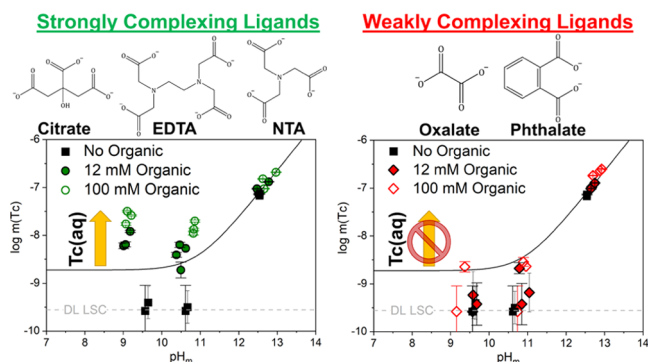
ABSTRACT: The chemistry of technetium ($t_{1/2}({}^{99}\text{Tc}) = 2.11 \times 10^5$ years) is of particular importance in the context of nuclear waste disposal and historic contaminated sites. Polycarboxylate ligands may be present in some sites and are potentially capable of strong complexing interactions, thus increasing the solubility and mobility of ${}^{99}\text{Tc}$ under environmentally relevant conditions. This work aimed to determine the impact of five organic complexing ligands [L = oxalate, phthalate, citrate, nitrilotriacetate (NTA), and ethylenediaminetetraacetate (EDTA)] under anoxic, alkaline conditions ($\text{pH} \approx 9\text{--}13$) on the solubility of technetium. X-ray absorption spectroscopy confirmed that $\text{TcO}_2(\text{am,hyd})$ remained the solubility-controlling solid phase in undersaturation solubility experiments. Ligands with maximum coordination numbers (CN) ≥ 3 (EDTA, NTA, and citrate) exhibited an increase in solubility from $\text{pH} 9$ to 11 , while ligands with $\text{CN} \leq 2$ (oxalate and phthalate) at all investigated pH and $\text{CN} \geq 3$ at $\text{pH} \approx 13$ were outcompeted by hydrolysis reactions. Though most available thermodynamic values were determined under acidic conditions, these models satisfactorily explained high- pH undersaturation solubility of technetium for citrate and NTA, whereas experimental data for $\text{Tc(IV)}\text{--EDTA}$ were highly overestimated. This work illustrates the predominance of hydrolysis under hyperalkaline conditions and provides experimental support for existing thermodynamic models of $\text{Tc}\text{--L}$ except $\text{Tc}\text{--EDTA}$, which requires further research regarding aqueous speciation and solubility.

KEYWORDS: technetium, organic, complexation, thermodynamics, solubility, redox

INTRODUCTION

Technetium (Tc) is a transition metal and the lightest element for which all isotopes are radioactive.¹ ${}^{99}\text{Tc}$ is a low-energy β emitter produced in appreciable quantities in nuclear reactors due to its relatively high fission yield ($\sim 6.0\%$) from ${}^{235}\text{U}$ and ${}^{239}\text{Pu}$ fuels.² Its predominance in spent nuclear fuel, radiotoxicity, and long half-life (211,100 years)³ combine to make technetium an element of concern for the long-term disposal of radioactive waste.

Technetium has complex chemistry which can determine its environmental mobility. Technetium has nine oxidation states ranging from $-I$ to VII , although only $+IV$ and $+VII$ are traditionally considered environmentally relevant. Tc(IV) is regarded as relatively immobile due to the formation of sparingly soluble $\text{TcO}_2(\text{am,hyd})$. Tc(VII) is remarkably mobile in comparison; Tc(VII) readily forms pertechnetate (TcO_4^-), which is stable under oxidizing to weakly reducing, aqueous conditions. Pertechnetate exhibits low sorption and high solubility characteristics, resulting in elevated mobility, thus causing pertechnetate to be a leading concern for the proper disposal of waste and the remediation of historic contaminated sites like the Hanford Site (Washington).⁴



Carboxylate-containing ligands are also expected to be present in specific waste streams, predominantly in low and intermediate level wastes (L/ILW). Oxalate ($\text{C}_2\text{O}_4^{2-}$) has been used in reprocessing schemes of spent nuclear fuel and is a major product from the radiolytic degradation of waste conditioning and ion-exchange materials.⁵ Phthalates ($\text{C}_8\text{H}_4\text{O}_4^{2-}\text{--R}_2$) are aromatic esters that are commonly used as PVC plasticizers and thus are expected to be present within specific L/ILW streams.⁶ These esters typically degrade to phthalic acid ($\text{C}_8\text{H}_6\text{O}_4$) over time, which is found as deprotonated phthalate ($\text{C}_8\text{H}_4\text{O}_4^{2-}$) in the alkaline to hyperalkaline conditions prevailing in repository systems. Citrate ($\text{C}_6\text{H}_5\text{O}_7^{3-}$), nitrilotriacetate (NTA, $\text{N}(\text{CH}_2\text{CO}_2)^{3-}$), and ethylenediaminetetraacetate (EDTA, $[\text{CH}_2\text{N}\text{--}$

$(\text{CH}_2\text{CO}_2)_2]_2^{4-}$) have all been used extensively in the nuclear industry as decontamination and separation agents.^{5,7-9}

These five ligands, illustrated in Figure S1, are of particular importance due to their carboxylate functional groups, which have been shown to favorably complex radionuclides like technetium under highly alkaline, anoxic conditions.⁵ Citrate also contains an alcohol group that has been shown to deprotonate at $\text{pH} > 12$ and participate in aqueous complex coordination in polynuclear complexes where steric hindrance is circumvented, thus increasing citrate's potential maximum coordination number (CN).⁵ Finally, NTA and EDTA contain one and two amine groups, respectively, which may also participate in lone-pair interactions. It is expected that as the maximum coordination number increases, the overall stability and thus solubility of the aqueous complex will also increase.

While investigations of technetium interactions with most of these ligands have been reported within the literature,⁹⁻¹⁵ a majority were conducted under acidic conditions and thus may not be representative of the type of complexes forming in alkaline systems. For instance, the strong hydrolysis of Tc(IV) results in the predominance of $\text{TcO}(\text{OH})_3^-$ at $\text{pH} \geq 10$, which may outcompete the formation of binary Tc(IV)-L complexes or contribute to the formation of ternary Tc(IV)-O/OH-L complexes. To better understand the overall chemistry of these metal-ligand complexes, it is imperative to look closer at technetium alkaline, aqueous complexation behavior in the presence of each of these polycarboxylate ligands.

In this work, we investigate the solubility, complexation, and redox behavior of technetium in the presence of a suite of chelating organic ligands which contain varying numbers of carboxylate functional groups. Experiments were performed under controlled redox conditions using a combination of undersaturation solubility experiments, oversaturation studies, and advanced spectroscopic techniques. This work aims to gain insight on the Tc-L complexes forming in alkaline to hyperalkaline conditions and investigate the applicability of available thermodynamic models, most of which were derived from experimental studies conducted under acidic to near-neutral pH conditions. From a more fundamental perspective, this work also aims at exploring the role of coordination number and number of carboxylate groups within an organic ligand on the thermodynamic stability of aqueous technetium complexes under conditions relevant for nuclear waste disposal.

THERMODYNAMIC BACKGROUND

Thermodynamic data considered in this work for aqueous complexes and solid compounds of technetium with inorganic ligands were taken from the ThermoChimie database and the recent update volume of the NEA-TDB dedicated to U, Np, Pu, Am, and Tc.^{16,17} An additional NEA-TDB volume by Hummel and co-workers focused on the aqueous complexation of radionuclides relevant to nuclear waste disposal by small organic ligands.⁵ Protonation constants for EDTA, citrate, and oxalate were taken from this review. NTA and phthalate thermodynamic constants were not included within this publication and thus were taken from other literature/database sources when available.^{10,17-19} Hummel and co-workers did not select any equilibrium constants for Tc(IV)-L complexes with the ligands investigated in this work. Due to this lack of selected data, thermodynamic values for Tc-L aqueous complexes were primarily taken from ThermoChimie.^{17,19}

ThermoChimie Selects a Single Formation Constant for Tc(IV)-EDTA. $\log K^\circ(\text{TcO}(\text{OH})(\text{EDTA})^{3-}) = (19.00 \pm 0.58)$ for the reaction $\text{TcO}(\text{OH})_2(\text{aq}) + \text{H}^+ + \text{EDTA}^{4-} \leftrightarrow \text{TcO}(\text{OH})(\text{EDTA})^{3-} + \text{H}_2\text{O}$.^{10,17,19} Additional studies^{11,12} reporting a similar formation constant ($\log K^\circ = 19.1$) were also discussed within the NEA-TDB⁵ but not selected due to insufficient redox control and unreported equilibration times. A more recent study¹³ proposed the formation of two Tc-EDTA complexes: $\log K^\circ(\text{TcO}(\text{EDTA})^{2-}) = (20.0 \pm 0.4)$ and $\log K^\circ(\text{Tc}(\text{OH})(\text{EDTA})^-) = (25.3 \pm 0.5)$. These values were later updated in another study¹⁴ ($\log K^\circ(\text{TcO}(\text{EDTA})^{2-}) = (17.9 \pm 0.3)$ and $\log K^\circ(\text{Tc}(\text{OH})(\text{EDTA})^-) = (20.5 \pm 0.1)$). Both publications reported that these complexes prevail in acidic to near-neutral pH conditions, but the reported stability constants were calculated using the TcO^{2+} moiety recently excluded in the NEA-TDB. For the sake of consistency between all Tc(IV)-L systems, and also considering the expected relevance in alkaline to hyperalkaline conditions, we use the $\text{TcO}(\text{OH})(\text{EDTA})^{3-}$ formation constant value selected by ThermoChimie for Tc(IV)-EDTA thermodynamic calculations herein.

ThermoChimie Selects Two Formation Constants for the Tc-NTA System. $\log K^\circ(\text{TcO}(\text{OH})(\text{NTA})^{2-}) = (13.30 \pm 0.32)$ and $\log K^\circ(\text{TcO}(\text{OH})(\text{NTA})_2^{5-}) = (11.70 \pm 0.50)$ for the reaction(s) $\text{TcO}(\text{OH})_2(\text{aq}) + \text{H}^+ + x\text{NTA}^{3-} \leftrightarrow \text{TcO}(\text{OH})(\text{NTA})_x^{(1-3x)} + \text{H}_2\text{O}$.^{10,17,19} Similar to Tc-EDTA, Tc-NTA formation constants have been studied more recently under acidic conditions and additional thermodynamic data have been reported.^{20,21} The NTA complex reported in these studies, $\text{TcO}(\text{NTA})^-$, forms only in acidic conditions, only conditional constants at $I \geq 0.5$ M NaNO_3 were provided, and equilibrium reactions were again defined using TcO^{2+} as master species. For these reasons, the values for Tc-NTA calculations within this work are sourced from ThermoChimie.

Tc-Oxalate Complexes with Stoichiometries 1:1 and 1:2 Are Selected within ThermoChimie. $\log K^\circ(\text{TcO}(\text{Ox})-\text{(aq)}) = (9.80 \pm 0.36)$ and $\log K^\circ(\text{TcO}(\text{Ox})_2^{2-}) = (13.66 \pm 0.37)$ for the reaction(s) $\text{TcO}(\text{OH})_2(\text{aq}) + 2\text{H}^+ + x\text{Ox}^{2-} \leftrightarrow \text{TcO}(\text{Ox})_x^{(2-2x)} + 2\text{H}_2\text{O}$.^{15,17,19} Tc-oxalate values within ThermoChimie were sourced from Xia et al.¹⁵ who performed a series of solvent extraction studies at $\text{pH} < 2$ to determine Tc-oxalate complex formation constants.

One Formation Constant for the Tc-Citrate System Selected from Wall et al.⁹ No values for Tc-citrate complexation were selected within ThermoChimie or discussed within the NEA-TDB. Wall et al.⁹ performed solvent extraction studies from $\text{pH} 4$ to 7 to determine the formation constants for two Tc-citrate complexes— $\text{TcO}(\text{OH})(\text{Cit})^{2-}$ and $\text{TcO}(\text{OH})_2(\text{Cit})^{3-}$ —which were subsequently corrected for ionic strength using the specific ion-interaction theory (SIT). The formation constants for these complexes were derived using the reactions $\text{TcO}(\text{OH})^+ + \text{Cit}^{3-} \leftrightarrow \text{TcO}(\text{OH})(\text{Cit})^{2-}$ and $\text{TcO}(\text{OH})_2(\text{aq}) + \text{Cit}^{3-} \leftrightarrow \text{TcO}(\text{OH})_2(\text{Cit})^{3-}$, respectively. $\text{TcO}(\text{OH})(\text{Cit})^{2-}$ has been disregarded in our solubility calculations because the $\text{TcO}(\text{OH})^+$ moiety is not consistent with the current NEA-TDB selection and the complex is only predominant at $\text{pH} < 6$, thus proving irrelevant for the experimental conditions investigated herein ($\text{pH} > 8$). Instead of calculating a model with both proposed complexes, only $\text{TcO}(\text{OH})_2(\text{Cit})^{3-}$ has been used for the solubility calculations within this work.

No Formation Constants Selected for Tc-Phthalate System. Finally, no thermodynamic values were found within the literature for technetium complexation with phthalate or any of its protonated forms. For this reason, the solubility data collected within this work are not compared to any calculated Tc-phthalate thermodynamic models. Most of the available thermodynamic values discussed within this section were determined using solvent extraction techniques conducted under primarily acidic conditions. Currently, limited literature is available regarding solubility studies, either from over- or undersaturation conditions, that have been performed to validate these solvent extraction-derived models under high-pH conditions. Thermodynamic models described above are used only for scoping calculations and qualitative comparison with experimental data obtained in this work. Development of fully consistent thermodynamic models involving NEA-TDB, ThermoChimie, and new experimental studies can only be achieved through the re-evaluation of available experimental data, which is outside of the scope of this work.

MATERIALS AND METHODS

Materials. Technetium experiments were performed in specialized laboratories in the controlled area of KIT-INE. All experiments were conducted in argon gloveboxes with $O_2 < 2$ ppm under carbonate exclusion. A previous study on the source and quantity of CO_2 within the current experiment type and setup suggests $CO_2 \leq (3.1 \pm 0.2) \times 10^{-5}$ M within Titrisol 1.0 M NaOH used for pH adjustment.²² All experimental solutions were prepared with ultrapure water purified with a Milli-Q apparatus (Millipore, 18.2 M Ω , 22 ± 2 °C). Before use, Milli-Q water was purged for at least 2 hours with argon gas. Ionic strength in NaCl (Merck, p.a.) experimental solutions was kept as low as possible ($I = 0.50$ – 0.85 M) while also attempting to maintain constant concentrations considering all solution components (i.e., Na_xH_yL -NaCl-NaOH-HCl-SnCl₂), described further below. NaOH and HCl solutions used for pH adjustments were prepared from standard solutions (Merck, Titrisol). Technetium solids and stock solutions were prepared from a chemically well-characterized ⁹⁹Tc stock solution (0.6 M NaTcO₄).²³

Preparation of TcO₂(am,hyd). The TcO₂(am,hyd) solid phase was prepared through electrochemical reduction and precipitation methods. Briefly, a 100 μ L aliquot of a ~ 0.6 M Tc(VII) stock solution was diluted in 25 mL of 1.0 M HCl before reduction with a platinum working electrode by applying a constant potential of -0.350 V (vs. SHE) through the use of an Ag/AgCl/3 M reference electrode and a standard Pt counter electrode. The three electrodes immersed in the diluted Tc(VII) solution were connected to a potentiostat (Princeton Applied Research Model 362) to control constant voltage. Following reduction and precipitation, the solid phase was washed with Milli-Q water and resuspended in a SnCl₂-containing solution.

Solubility Experiments. Batch-type undersaturation solubility experiments using TcO₂(am,hyd) were carried out at constant ligand concentrations (12, 100 mM) and constant pH_m (9, 11, 13). SnCl₂ (2 mM) was implemented as a redox buffer to ensure strongly reducing conditions in all batch reactors. Although traces of Sn(IV) probably formed in the course of the experiments, the very low (pe + pH) values retained throughout the experiments indicated that Sn was mostly found in the +II oxidation state (see discussion in the

Supporting Information). The lowest organic concentration (targeted at 10 mM) was increased to 12 mM to account for any potential Sn(II)- or Sn(IV)-ligand complexation which may occur. Table S1 details the experimental conditions for each individual batch experiment. TcO₂(am,hyd) (~ 1.5 mg) was added to batch reactors through a procedure involving centrifugation of the solid suspension, washing of the solid phase with Milli-Q water, and resuspension in the experimental solution.

Batch-type oversaturation experiments using aqueous NaTcO₄ stock solutions were carried out at constant ligand concentration (100 mM) and constant pH_m (9, 11, 13). Two pertechnetate (TcO₄⁻) concentrations were implemented at each pH_m: 10^{-3} and 10^{-5} M. SnCl₂ (2 mM) was used as a redox buffer in most batch reactors; additional experiments at pH_m ~ 13 were performed without any SnCl₂ inclusion as a control to investigate the role of reducing conditions on technetium oversaturation solubility over time. Table S2 details the experimental conditions for each individual batch experiment. TcO₄⁻ was added to experimental solutions through a procedure involving 10 kD ultrafiltration of the ~ 0.6 M NaTcO₄ stock solution, dilution of the filtered stock to an appropriate intermediate concentration with Milli-Q water, and then spiking an aliquot of the diluted stock into experimental solutions to achieve the targeted TcO₄⁻ concentrations.

Ionic strength in all systems was targeted at ~ 0.5 M while accounting for the contribution of all of the components (e.g., Na₄EDTA-Na₃HEDTA-Na₂H₂EDTA-NaH₃EDTA-H₄EDTA-NaCl-HCl-NaOH). However, due to the large negative charges on many of the ligands at high pH, actual I varied from 0.50 to 0.85 M. The pH_m of each sample was adjusted using appropriate concentration solutions of HCl and NaOH to maintain the targeted ionic strength before technetium addition. After technetium addition, samples were shaken on a semiregular, weekly basis and experimental pH_m, E_h , and aqueous technetium concentrations (after 10 kD ultrafiltration) were monitored in all undersaturation and oversaturation systems for ≤ 278 or ≤ 173 days, respectively.

Analytical Methods. All pH measurements were performed using combination pH electrodes (Orion Ross, Thermo Scientific) calibrated against standard pH buffers (pH = 7–12, Merck). Herein, we report pH as pH_m or the total free concentration of protons in molal units. In salt solutions of ionic strength (I) ≥ 0.1 mol·kg⁻¹, the measured pH value (pH_{exp}) is an operational apparent value related to m_{H^+} by $pH_m = pH_{exp} + A_m$, where A_m accounts for the activity coefficient of H⁺ and the liquid junction of the electrode at the given NaCl concentration.²⁴ Redox potentials of experimental solutions containing redox buffers were determined using combination Pt, Ag/AgCl reference electrodes (Metrohm). Further description of these measurement methods and subsequent calculations to determine pH_m and E_h /pe can be found within the literature.^{25,26}

A PerkinElmer Quantulus liquid scintillation counter (LSC) was used to determine total aqueous technetium concentrations. LSC samples were prepared through 10 kD ultrafiltration (2–3 nm, Pall Life Sciences) and subsequent mixing with 10 mL of PerkinElmer Ultima Gold XR LSC cocktail. Samples were counted for a minimum of 30 min to achieve satisfactory counting statistics. Preliminary experiments determined that none of the ligands utilized within this study

exhibited quenching effects on the technetium LSC signal, thus verifying the procedure and use of LSC throughout this study.

X-ray Absorption Spectroscopy (XAS). Technetium K-edge X-ray absorption near-edge structure (XANES) and extended X-ray absorption fine structure (EXAFS) spectra were recorded at the KIT light source (KARA storage ring, KIT Campus North) using the ACT station of the CAT-ACT beamline.²⁷ The storage ring operated at 2.5 GeV electron energy with a mean electron current of 120 mA. The standard beam size and flux at the sample position were $\sim 1 \times 1$ mm and ~ 1011 photons \cdot s $^{-1}$ per 100 mA at 20 keV, Si(111), respectively. Solid phases were retrieved and characterized by EXAFS to verify the structure of the solubility-controlling solid phase in undersaturation experiments. X-ray absorption spectroscopy (XAS) spectra of the technetium K-edge (21,044 eV) were recorded in both fluorescence and absorbance detection modes using an 8-pixel LEGe solid-state detector and argon-filled ionization chambers. Incident beam intensity and the transmission of 20 μ m molybdenum metal reference foil were recorded simultaneously using an argon-filled ionization chamber at ambient pressure. Technetium solid phases were measured in sealed polyethylene sample containers equipped with a Kapton window and sealing O-ring; all encased in a secondary sealed bag with an additional Kapton window flushed with argon gas. Aliquots of a solid suspension were prepared for analysis within an argon atmosphere glovebox following centrifugation and washing with degassed Milli-Q water.

EXAFS data reduction was performed with the ATHENA and ARTEMIS software from the Demeter 0.9.26 program package²⁸ following standard procedures. Spectra were calibrated against the first inflection point in the molybdenum reference foil K-edge spectrum (20,000 eV), and E_0 for the technetium K-edge was selected at the first inflection point of the white line using the first derivative. Tc(VII) and TcO₂(am,hyd) reference spectra were collected under similar experimental conditions for comparison. EXAFS data analysis was based on standard least-squares fit techniques while neighbor atom distances (R_i), Debye–Waller factors (σ_i^2), and coordination numbers (N_i) for different coordination shells (i) were determined using the FEFFIT code (FEFF6) within the program package to derive ab initio scattering amplitudes and phase shifts. The crystallographic information file (COD:4124108) for the structure of TcO₂ was obtained from Rodriguez et al.²⁹ Fit operations were performed in R -space and the amplitude reduction factor (S_0^2) was fixed at 0.75, which was determined by fitting the TcO₄⁻ reference spectrum with fixed $N = 4.0$.

Data Analysis and Modeling Methods. Thermodynamic calculations in this work are based on the reactions and associated constants provided in Table S3. SIT was used for ionic strength corrections,³⁰ and ion-interaction parameters (Table S4) were either taken from the literature^{5,16} or estimated based on Hummel’s charge correlation approach.³¹ The Medusa/Spina^{32,33} software package was applied for data analysis/modeling, solubility, and Pourbaix (pe-pH_m) diagram calculations. Thermochemical models were calculated with $I = 0.7$ M NaCl to best represent the average ionic strength across all experimental reactors.

RESULTS AND DISCUSSION

Undersaturation Solubility Experiments. Experimentally measured pH_m and pe values from undersaturation

solubility experiments are plotted on the Pourbaix diagram in Figure S2, which displays the calculated predominance fields of technetium solid compounds and aqueous species in ligand-free systems. The comparison of experimental pH_m and pe values with the thermodynamic calculations shows that all undersaturation solubility experiments maintained significantly reducing conditions, as expected through the implementation of SnCl₂ as a redox buffer (pe + pH_m \approx 1.50). This implies that both aqueous and solid technetium are expected to be Tc(IV), at least in the absence of any organic ligand. Additionally, Figure S3 shows the XANES spectrum of a selected solid phase as compared to reference Tc(IV) and Tc(VII) spectra, providing further evidence for technetium in the +IV oxidation state within experimental solids.

EXAFS analysis was also performed on a selected solid phase to verify the integrity of the solid over the experimental lifetime. Figure 1 shows the Fourier-transformed (FT)

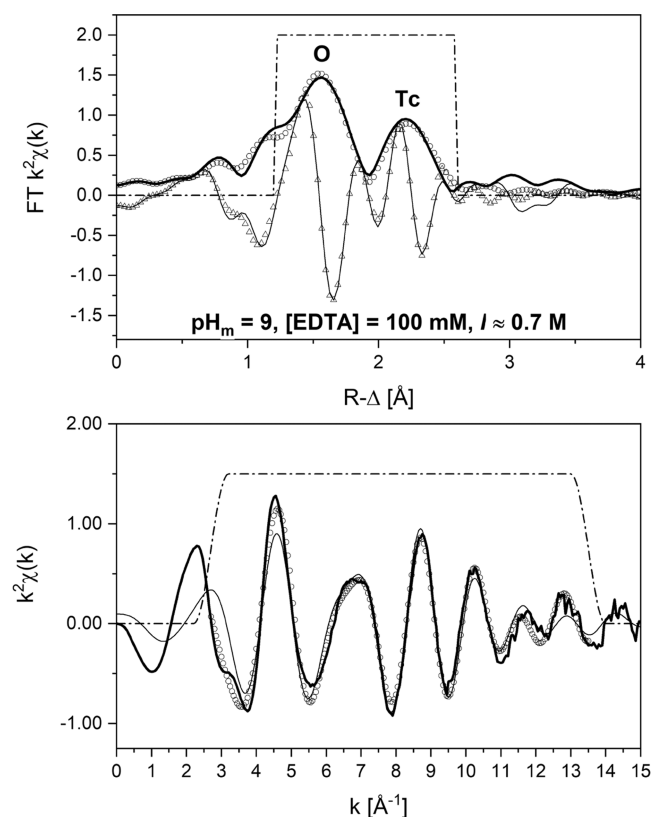


Figure 1. Technetium K-edge EXAFS fit results for the Tc^{IV}O₂(am,hyd) solid phase recovered from the undersaturation system in the presence of 100 mM EDTA—upper panel: FT magnitude (solid line), fit magnitude (open circles), FT real part (thin solid line), and fit real part (open triangles); lower panel: Fourier-filtered data (solid line), raw data (thin solid line), and back-transformed fit (open circles). R - and k -range fitting windows are represented by dashed lines.

representation of k^2 -weighted EXAFS data for solid phase recovered from the 100 mM EDTA system at pH_m \sim 9. This solid phase was chosen for EXAFS measurements because the 100 mM EDTA system at pH_m \sim 9 exhibited the highest amount of dissolution of all investigated systems. The data set was fit with two coordination shells and structural parameters resulting from the fit of the EXAFS spectrum are summarized in Table 1. During fitting and interpretation of the EXAFS

Table 1. Data Range and Parameters Generated by Least-Squares Fitting of EXAFS Spectra^a

sample	k -range (\AA^{-1})	fit-range (\AA)	path	N	R (\AA)	ΔE_0 (eV)	σ^2 (\AA^2)	r -factor (%)
$\text{pH}_m \approx 9$		2.7–13.5	Tc–O	5.4	2.04	3.139	0.0025 ^c	1.8
[EDTA] = 100 mM		1.2–2.6	Tc–Tc	2.0 ^b	2.58		0.0035 ^c	

^a $S_0^2 = 0.75$, as determined from TcO_4^- reference analysis (Tc–O N fixed to 4.0). Fit errors: CN: $\pm 20\%$, R : 0.01 \AA , σ^2 : 0.001 \AA^2 . ^bHeld constant during the fit. ^cConstrained during the fit.

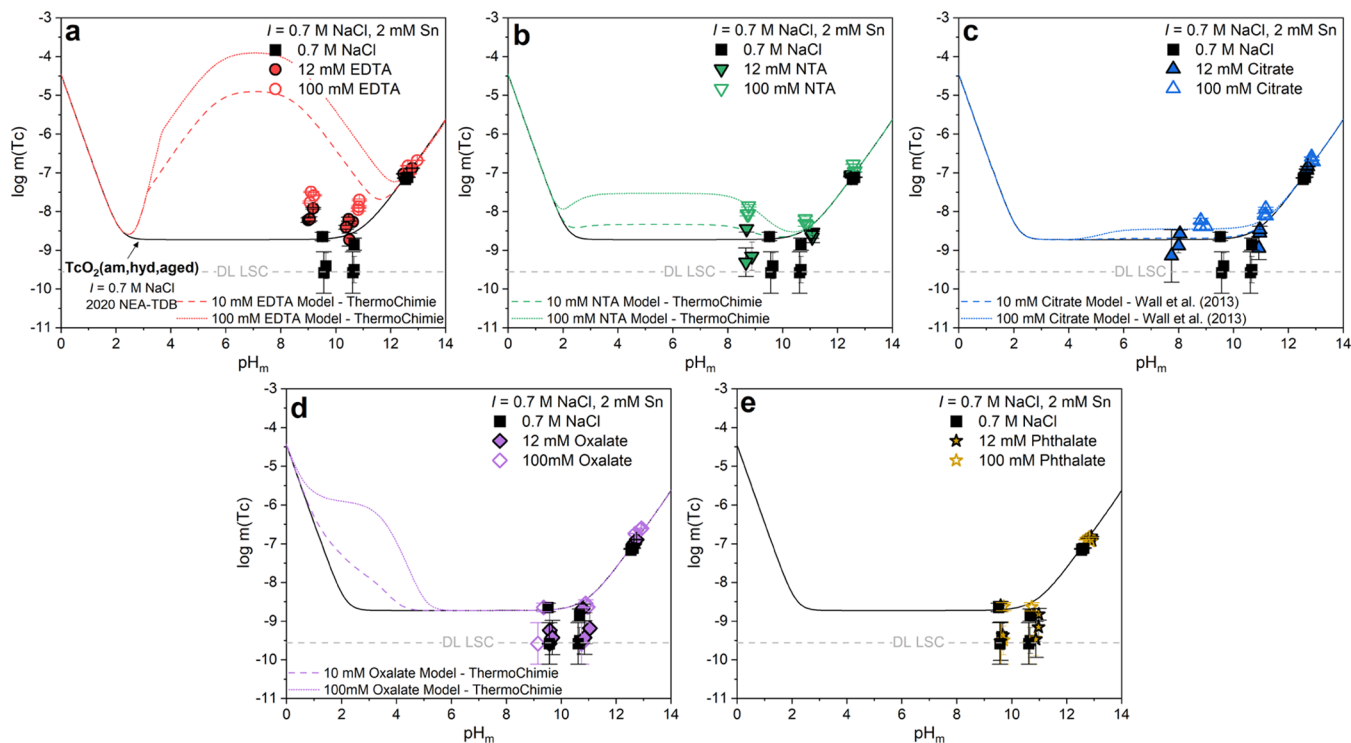


Figure 2. Experimentally measured $m(\text{Tc})_{\text{tot}}$ in equilibrium with $\text{TcO}_2(\text{am,hyd})$ at $[L]_{\text{tot}} = 0, 12, \text{ or } 100 \text{ mM}$ and $I \approx 0.7 \text{ M NaCl-HCl-NaOH-Na}_x\text{L}$ for undersaturation experiments with $L =$ (a) EDTA, (b) NTA, (c) citrate, (d) oxalate, and (e) phthalate. All data were collected between 41 and 278 days of equilibration, except for EDTA, which only shows data collected after 76 days of equilibration. Solid and dotted lines correspond to the thermodynamically calculated solubility of $\text{TcO}_2(\text{am,hyd})$ under different solution conditions based on values from the literature (Table S3).^{9,10,15–17} Gray dashed lines represent the LSC detection limits (DL LSC) for the experimental analyses, and all error bars are either represented or contained within data symbols.

data, many different optimizations and models were attempted to best represent the solid-phase data, but the fitting model represented in the literature³⁴ which holds the Tc–Tc shell constant at 2, combined with the use of a $\text{TcO}_2 \cdot x\text{H}_2\text{O}$ CIF, resulted in the best fit of our data and the most realistic generated parameters. This also allowed for a more direct comparison to parameters reported within literature sources. The EXAFS fit of the solid phase shows an O-shell at 2.04 \AA with a coordination number $N_{\text{O}} = 5.4$ and a Tc shell at 2.58 \AA with $N_{\text{Tc}} = 2$. These results are in good agreement with structural parameters reported in the literature for hydrated TcO_2 (i.e., $\text{TcO}_2 \cdot x\text{H}_2\text{O}$ or $\text{TcO}_2(\text{am,hyd})$),^{29,34,35} thus providing evidence that $\text{TcO}_2(\text{am,hyd})$ remained the solubility-controlling solid phase throughout the lifetime of the undersaturation solubility experiments.

Figure 2 shows the experimentally determined molal aqueous technetium concentrations ($m(\text{Tc})_{\text{tot}}$) for experiments of $\text{TcO}_2(\text{am,hyd})$ equilibrated in solutions of 0, 12, or 100 mM total ligand concentration ($[L]_{\text{tot}}$), $I \approx 0.7 \text{ M NaCl-HCl-NaOH-Na}_x\text{L}$, and 2 mM SnCl_2 at steady state as compared to literature thermodynamic models.^{9,10,15,17,19} Steady state was achieved for all undersaturation experiments within <112 days (see Figure S4).

Control data in the absence of any ligand was well represented by the $\text{TcO}_2(\text{am,hyd})$ solubility model (Figure 2a–e, black squares). This model displays limited solubility in the circumneutral to slightly alkaline range ($\log m(\text{Tc})_{\text{tot}} \approx -8.7$), followed by a significant increase of ~ 2.5 orders of magnitude as pH_m increases from 10 to 14. The reason for the increase in $m(\text{Tc})_{\text{tot}}$ is the equilibrium between the two solubility reactions $\text{TcO}_2(\text{am,hyd}) + 2\text{H}_2\text{O}(\text{l}) \leftrightarrow \text{TcO}(\text{OH})_2(\text{aq})$ and $\text{TcO}_2(\text{am,hyd}) + 3\text{H}_2\text{O}(\text{l}) \leftrightarrow \text{TcO}(\text{OH})_3^- + \text{H}^+$, which reflect the predominance of $\text{TcO}(\text{OH})_2(\text{aq})$ under circumneutral/slightly alkaline conditions and the ingrowth of the $\text{TcO}(\text{OH})_3^-$ complex with elevated pH (i.e., 10–14). The excellent agreement between our experimental data in the absence of ligands and the calculated solubility verifies both the precision and reproducibility of our experimental methods and the chosen solubility models for the basis of further modeling calculations within this work.

When comparing aqueous technetium concentrations in the presence and absence of ligands, a clear separation occurred between strongly and weakly complexing ligands. Only three of the five selected organic ligands—EDTA, NTA, and citrate—resulted in an increase in $m(\text{Tc})_{\text{tot}}$ (Figure 2a–c), while the other two ligands—oxalate and phthalate—displayed trends

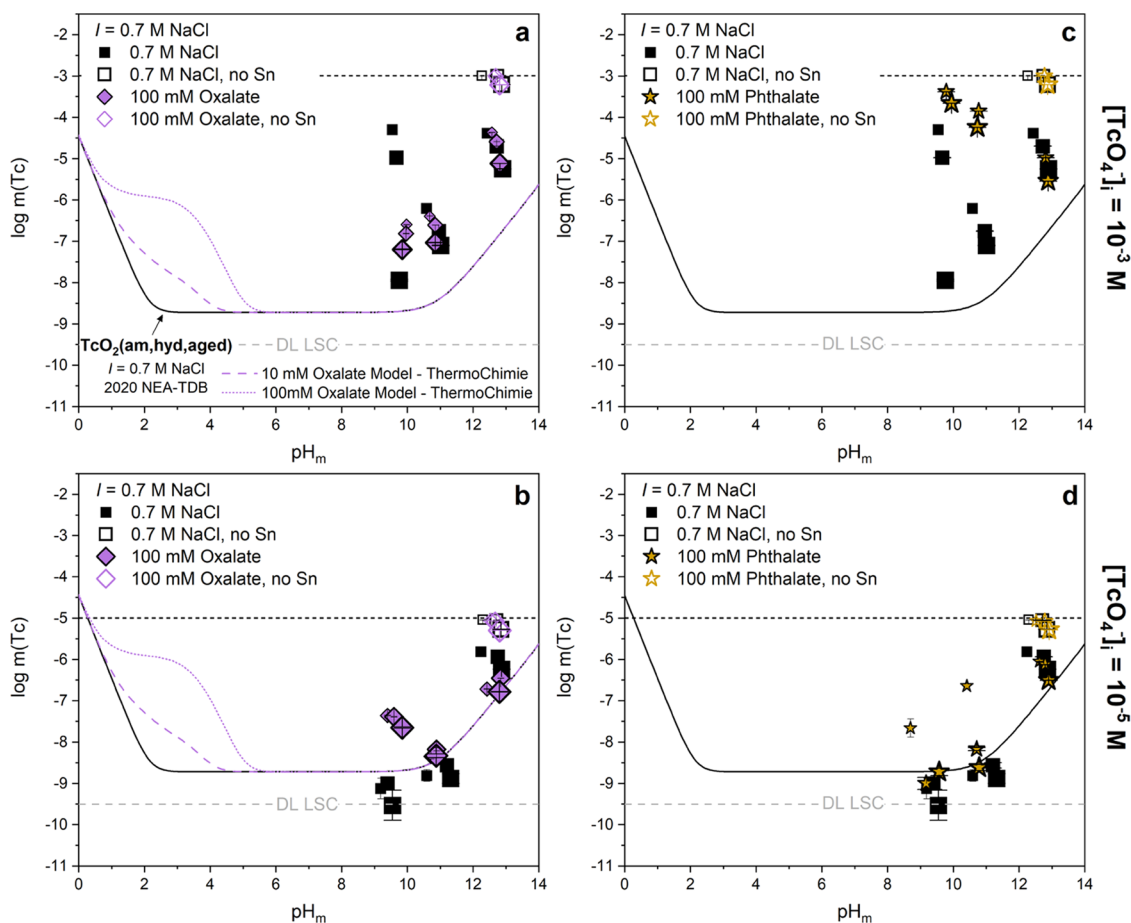


Figure 3. Oversaturation experimentally measured aqueous $m(\text{Tc})_{\text{tot}}$ at $[\text{L}]_{\text{tot}} = 0 \text{ M}$ (black squares) or 100 mM (colored symbols) in the presence (solid symbols) or absence (open symbols) of SnCl_2 with $[\text{TcO}_4^-]_i = 10^{-3} \text{ M}$ (top panel) or 10^{-5} M (bottom panel) where $L = (\text{a, b})$ oxalate and (c, d) phthalate. Data points increase in size with increasing equilibration time: $t_1 = 41$ days, $t_2 = 88$ days, and $t_3 = 173$ days. Solid and dotted lines correspond to the thermodynamically calculated solubility of $\text{TcO}_2(\text{am,hyd,aged})$ under different solution conditions based on values from the literature (Table S3).^{9,10,15–17} Gray dashed lines represent the LSC detection limits for the experimental analyses, and all error bars are either represented or contained within data symbols.

nearly identical to the ligand-free control experiments (Figure 2d,e).

Experiments containing oxalate or phthalate at both $[\text{L}]_{\text{tot}} = 12$ and 100 mM did not exhibit an increase in $m(\text{Tc})_{\text{tot}}$ when compared to control experiments. This indicates that if $\text{Tc(IV)}\text{-L}$ complexation occurred for oxalate and phthalate systems, these complexes did not become predominant at pH_m 9–13. It appears evident that both ligands are not strong enough complexants to outcompete hydrolysis reactions under alkaline conditions. Results obtained for $\text{Tc(IV)}\text{-oxalate}$ experiments were in line with current thermodynamic calculations, which only predict elevated solubility through Tc-Ox aqueous complexation (i.e., $\text{TcO}(\text{ox})(\text{aq})$ and $\text{TcO}(\text{ox})_2^{3-}$ formation) up to pH values of 5–6 and no increase in solubility resulting from Tc-Ox complex formation at higher pH, such as the pH ranges utilized within our experiments. Note, however, that the solvent extraction study by Xia et al.¹⁵ was performed at $\text{pH} \sim 1.5$. As previously discussed, no current thermodynamic model could be found for the $\text{Tc(IV)}\text{-phthalate}$ system, so a similar model comparison could not be performed.

For systems containing strongly complexing ligands—EDTA, NTA, and citrate—elevated $m(\text{Tc})_{\text{tot}}$ was observed at both $\text{pH}_m \sim 9$ and ~ 11 while little to no increase in $m(\text{Tc})_{\text{tot}}$

occurred at $\text{pH}_m \sim 13$. For less alkaline samples, the increase in $m(\text{Tc})_{\text{tot}}$ further increased with larger ligand concentrations. This strongly supports the formation of $\text{Tc}(\text{OH})\text{-L}$ complexes in solution. Experimental observations at $\text{pH}_m \sim 13$ indicate that $\text{Tc}(\text{OH})\text{-L}$ complexes cannot outcompete the predominance of the $\text{TcO}(\text{OH})_3^-$ hydrolysis species, at least in the range of ligand concentrations investigated in this work. The increased $m(\text{Tc})_{\text{tot}}$ observed for NTA and citrate experiments was well-described by the selected thermodynamic models (see the Thermodynamic Background section). These calculations effectively described not only the increase in $m(\text{Tc})_{\text{tot}}$ as a function of pH_m but also the differences in $m(\text{Tc})_{\text{tot}}$ at different $[\text{L}]_{\text{tot}}$, thus providing additional experimental support for the selected $\text{Tc(IV)}\text{-NTA}$ and $\text{Tc(IV)}\text{-citrate}$ formation constants (Table S3).

Alternatively, the thermodynamic model for the $\text{Tc(IV)}\text{-EDTA}$ system overestimates experimental $m(\text{Tc})_{\text{tot}}$ at $\text{pH}_m \sim 9$ and ~ 11 for both $[\text{EDTA}]_{\text{tot}} = 12$ and 100 mM by 1–3 orders of magnitude. The original source for the $\log \beta^\circ(\text{TcO}(\text{OH})\text{-EDTA}^{3-})$ value selected in ThermoChimie is the ion-exchange study by Gorski and Koch.¹¹ This study was performed at $\text{pH} \sim 1.5$ without any specific control of the redox conditions (possibly under air). Conducting experiments at constant pH typically prevents the unequivocal definition of

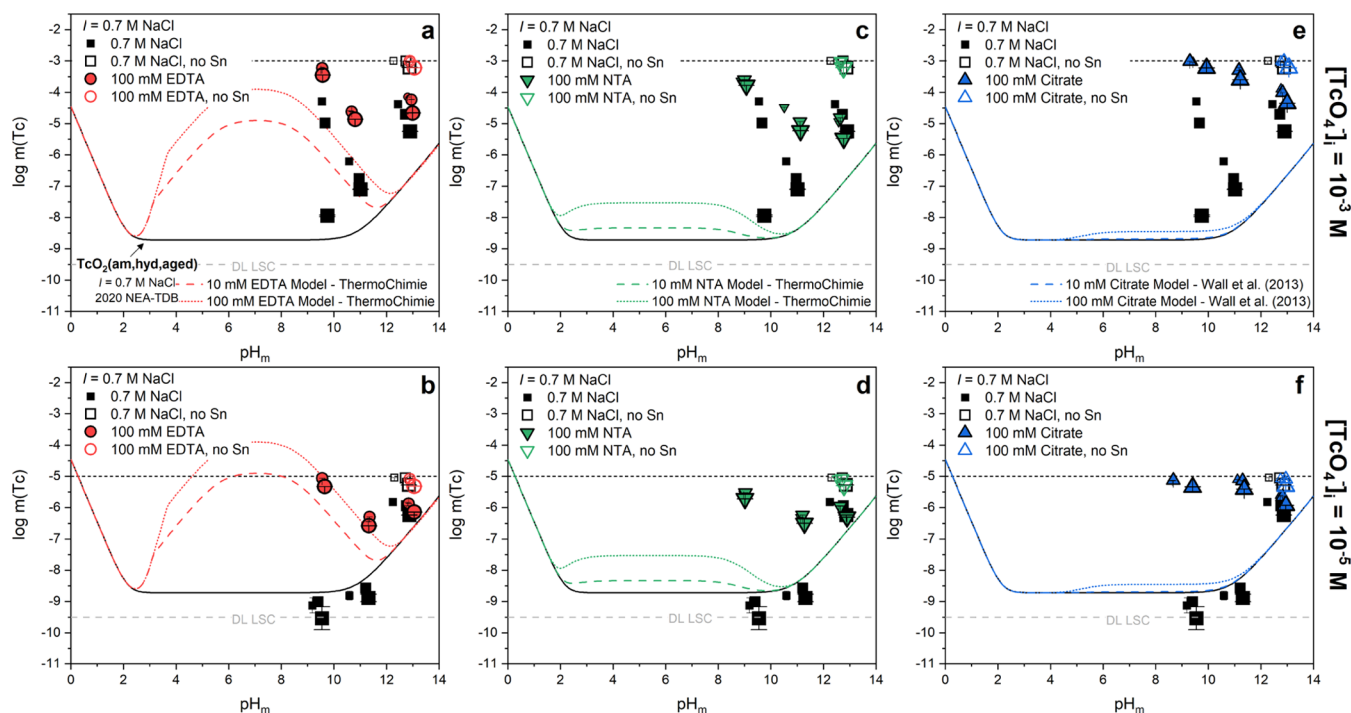


Figure 4. Oversaturation experimentally measured aqueous $m(\text{Tc})_{\text{tot}}$ at $[L]_{\text{tot}} = 0 \text{ M}$ (black squares) or 100 mM (colored symbols) in the presence (solid symbols) or absence (open symbols) of SnCl_2 with $[\text{TcO}_4^-]_i = 10^{-3} \text{ M}$ (top panel) or 10^{-5} M (bottom panel) where $L =$ (a, b) EDTA, (c, d) NTA, and (e, f) citrate. Data points increase in size with increasing equilibration time: $t_1 = 41$ days, $t_2 = 88$ days, and $t_3 = 173$ days. Solid and dotted lines correspond to the thermodynamically calculated solubility of $\text{TcO}_2(\text{am,hyd})$ under different solution conditions based on values from the literature (Table S3).^{9,10,15–17} Gray dashed lines represent the LSC detection limits for the experimental analyses, and all error bars are either represented or contained within data symbols.

complex stoichiometry, and the lack of redox control may have resulted in the (partial) oxidation of Tc(IV) to Tc(VII). Furthermore, experiments by Gorski and Koch¹¹ were performed within a timeframe of 3 hours, which may prove insufficient to attain equilibrium conditions in the Tc(IV)–EDTA system. In fact, steady-state conditions in some of the solubility samples investigated in this work were only attained after 41 days (see Figure S5). Thus, in line with the argumentation provided by NEA-TDB reviewers and outlined herein, we consider the model provided by Gorski and Koch as not fully reliable, especially for extrapolation to elevated pH systems. Therefore, Tc(IV)–EDTA thermodynamic values need to be revisited on the basis of new, systematic experimental studies.

Oversaturation Experiments. Experimentally determined pH_m and pe values from oversaturation solubility experiments are plotted on the Pourbaix diagrams in Figure S6 together with calculated predominance fields of technetium solid compounds and aqueous species. While we observed larger variation in experimental pe measurements compared to undersaturation experiments, specifically at $\text{pH}_m \sim 9$, it is clear that the Sn-containing solutions maintained significantly reducing conditions, even if a fraction of the Sn(II) was potentially oxidized to Sn(IV). Measurements of pe in the absence of a redox buffer are generally considered less reliable due to undefined redox couples within solution, but qualitatively we observed an increased pe for the experiments in the absence of SnCl_2 compared to those containing SnCl_2 at the same pH_m .

Figures 3 and 4 show comparisons of experimentally determined $m(\text{Tc})_{\text{tot}}$ from oversaturation solubility experiments in the presence of weakly and strongly complexing

ligands, respectively. Oversaturation experiments were conducted using two different starting concentrations of Tc(VII) ($[\text{TcO}_4^-]_i = 10^{-3}$ and 10^{-5} M). Experiments conducted in the absence of SnCl_2 and ligand-free experiments were performed as controls to determine the impact of reducing conditions and ligand complexation on the oversaturation solubility of technetium over time (≤ 173 days), respectively.

For all experiments in the absence of SnCl_2 , no decrease in $m(\text{Tc})_{\text{tot}}$ was observed over time. This indicates that reducing conditions, and the subsequent reduction to Tc(IV), are necessary to induce a decrease in technetium solubility. This is supported through a wide range of studies in the literature characterizing pertechnetate as highly stable, soluble, and mobile in oxidizing, aqueous environments.² The observed continued persistence of elevated technetium concentrations in solution also suggests that in the absence of reducing conditions, all five organic ligands investigated within this study do not appear to have a significant reducing effect on technetium.

A decrease in $m(\text{Tc})_{\text{tot}}$ was observed over time for experiments conducted in the presence of SnCl_2 but in the absence of any ligand. Long-term $m(\text{Tc})_{\text{tot}}$ were lowest at $\text{pH}_m \sim 9$ and highest at $\text{pH}_m \sim 13$, as expected from the calculated ligand-free solubility of $\text{TcO}_2(\text{am,hyd})$. The $m(\text{Tc})_{\text{tot}}$ for both $[\text{TcO}_4^-]_i = 10^{-3}$ and 10^{-5} M systems approached the thermodynamically calculated solubility of $\text{TcO}_2(\text{am,hyd})$ over time, but due to lower initial technetium concentrations, the 10^{-5} M system approached this solubility limit more quickly than the 10^{-3} M system. We hypothesize that if these systems were monitored further, ligand-free oversaturation experiments would have achieved $m(\text{Tc})_{\text{tot}}$ concentrations equivalent to the selected thermodynamic model.

Experiments conducted in the presence of organic complexing ligands again exhibited a split in solubility trends between weakly complexing ligands—oxalate and phthalate—and strongly complexing ligands—EDTA, NTA, and citrate. Figure 3 displays the oversaturation solubility data for weakly complexing ligands. For both ligands, we observed a decrease in $m(\text{Tc})_{\text{tot}}$ over time, similar to ligand-free experiments. Lower concentration experiments ($[\text{TcO}_4^-]_i = 10^{-5} \text{ M}$) for both weakly complexing ligands were either the same as or approaching similar $m(\text{Tc})_{\text{tot}}$ to undersaturation solubility experiments, suggesting that these systems are close to achieving equilibrium. Phthalate experiments at $[\text{TcO}_4^-]_i = 10^{-3} \text{ M}$ exhibited higher $m(\text{Tc})_{\text{tot}}$ than oxalate experiments, but both still displayed consistent decreases in concentration at each sampling time point and would likely approach the $m(\text{Tc})_{\text{tot}}$ observed in ligand-free experiments if observed over longer time periods. This suggests that while both ligands can be considered weakly complexing, they may exhibit slightly different kinetics at elevated Tc concentrations or may even proceed through different reaction mechanisms before Tc precipitation. These data and the suggestion of an equilibrium between over- and undersaturation conditions provide further support for the conclusion that if Tc(IV)–oxalate or Tc(IV)–phthalate complexes formed under the investigated conditions, they did not become the predominant species in solution within our experiments.

Strongly complexing ligands led to an even slower decrease of the initial Tc concentration (Figure 4). The decrease in Tc concentration observed in most of the systems can only be explained with the precipitation of a Tc(IV) solid phase (expectedly $\text{TcO}_2(\text{am,hyd})$) after the reduction of Tc(VII) to Tc(IV) in the aqueous phase. Two main hypotheses can be raised to explain the very slow precipitation kinetics: (i) formation of polynuclear complexes, likely triggered by the presence of hydroxo groups in ternary Tc(IV)–OH–L moieties, and (ii) formation of a transient state involving the presence of other oxidation states of Tc, likely Tc(V)–L. In our previous study with gluconate, a chelating ligand with one carboxylic and five alcohol groups, oversaturation experiments with Tc(VII) in the presence of SnCl_2 as a reducing agent resulted in even slower precipitation kinetics than those observed in the present study for EDTA, NTA, and citrate.³⁶ In the Tc–gluconate system, Tc K- and L_3 -edge XANES confirmed that in the presence of the Sn reducing agent, Tc was exclusively found in the +IV oxidation state, but in the absence of any Sn reducing agent, the +V oxidation state was observed. It is notable, as well, that the formation of colloidal/polynuclear species further stabilized by inorganic (e.g., CO_3^{2-}) or organic ligands (e.g., isosaccharinic acid) has been previously described for other tetravalent elements such as the actinides.^{37–39} A long-term study with Tc–citrate and Tc–EDTA systems from oversaturation conditions involving Tc K- and L_3 -edge XANES is currently ongoing in an attempt to characterize the chemistry occurring in these systems more definitively, and the main findings will be summarized in a separate publication. Although this ongoing study will help to unravel the chemistry of technetium in the transient state, the results obtained in the present study strongly point to an end point defined by Tc(IV) aqueous complexes and solid compounds in the very reducing conditions investigated in this work.

Applicability within Environmental Systems. This work presents an investigation of alkaline and hyperalkaline

solubility data from both undersaturation and oversaturation conditions and subsequent comparison to available thermodynamic data for Tc(IV)–L systems within the literature (L = EDTA, NTA, citrate, oxalate, and phthalate). Undersaturation conditions were investigated to glean information regarding thermodynamic equilibrium, as these conditions normally promote relatively quick equilibration and limited variation in experimental conditions over time. Oversaturation conditions were implemented to further investigate redox contributions and potential transience within Tc–L systems.

Currently, most available thermodynamic models within the literature were derived from studies conducted under acidic conditions. Thus, experimental comparisons to these thermodynamic values are necessary to truly establish equilibrium speciation of Tc(IV) under conditions relevant for nuclear waste disposal. Five organic ligands containing 2–4 carboxylate groups, along with additional alcohol and amine functional groups, were investigated to determine the impact of coordination number and additional functional groups on overall technetium solubility, as well.

The two weakly complexing ligands with predicted coordination numbers (CN) ≤ 2 —oxalate and phthalate—were found to have limited effects on overall technetium solubility from pH_m 9 to 13. As neither over- nor undersaturation studies exhibited a clear increase in solubility with respect to ligand-free control experiments, it was determined that if Tc(IV)–oxalate or Tc(IV)–phthalate complexes do form, they do not become the predominant, solubility-controlling species in alkaline solutions. Likely, these complexes are outcompeted by the formation of Tc(IV)–hydrolysis species under high-pH conditions.

All three strongly complexing (CN ≥ 3) ligands—EDTA, NTA, and citrate—exhibited a clear impact on aqueous technetium solubility. From undersaturation conditions, this increase in solubility was well-described by current NTA and citrate thermodynamic models, but not well-described for the EDTA systems. From oversaturation conditions, all three systems maintained elevated aqueous technetium concentrations with little to no variation over time indicating the formation of a potential metastable state (i.e., potential stabilization of different technetium moieties than those included within the models). In line with previous studies with the Tc–gluconate system, this work supports that very slow precipitation kinetics occur in the presence of chelating ligands with CN ≥ 3 .

Ultimately, this work has shown that under hyperalkaline conditions, such as those which would be expected in cementitious, nuclear waste disposal scenarios, hydrolysis is expected to compete with both strongly and weakly complexing organic ligands investigated within this study. From this work, we would expect the investigated organic complexing ligands to show a limited impact on the overall solubility and mobility of technetium in long-term disposal scenarios in repositories for L/ILW.

ASSOCIATED CONTENT

● Supporting Information

Figure showing the structures of the organic ligands; tables of the experimental conditions; tables of all thermodynamic constants used within this work; figures

showing the redox conditions of the experiments; figure showing the XANES data for the TcO₂ solid phase; figure showing the short time point data for the 100 mM EDTA system; and detailed description of the role of Sn(II/IV) and Sn(II/IV)–EDTA complexes within the investigated systems with corresponding figures and tables of thermodynamic constants (PDF)

AUTHOR INFORMATION

Corresponding Authors

Nicole A. DiBlasi – Karlsruhe Institute of Technology, Institute for Nuclear Waste Disposal, Eggenstein-Leopoldshafen 76344, Germany; orcid.org/0000-0003-4385-0438; Email: nicole.a.dibiasi@gmail.com

Xavier Gaona – Karlsruhe Institute of Technology, Institute for Nuclear Waste Disposal, Eggenstein-Leopoldshafen 76344, Germany; Email: xavier.gaona@kit.edu

Authors

Kathy Dardenne – Karlsruhe Institute of Technology, Institute for Nuclear Waste Disposal, Eggenstein-Leopoldshafen 76344, Germany

Tim Prüssmann – Karlsruhe Institute of Technology, Institute for Nuclear Waste Disposal, Eggenstein-Leopoldshafen 76344, Germany; orcid.org/0000-0002-7903-9199

Sarah Duckworth – Karlsruhe Institute of Technology, Institute for Nuclear Waste Disposal, Eggenstein-Leopoldshafen 76344, Germany

Marcus Altmaier – Karlsruhe Institute of Technology, Institute for Nuclear Waste Disposal, Eggenstein-Leopoldshafen 76344, Germany

Notes

The authors declare no competing financial interest. The authors declare that they have no known competing financial interests or personal relationships that could have appeared to influence the work reported in this paper.

ACKNOWLEDGMENTS

The KIT Institute for Beam Physics and Technology (IBPT) is acknowledged for the operation of the storage ring, the Karlsruhe Research Accelerator (KARA), and provision of beamtime at the INE and ACT Beamlines operated by the Institute for Nuclear Waste Disposal at the KIT light source. This work was partly funded by the German Federal Ministry for Economic Affairs and Climate Action (BMWK) within the framework of the VESPAII project (contract number 02E11607C).

REFERENCES

- (1) Perrier, C.; Segrè, E. Some Chemical Properties of Element 43. *J. Chem. Phys.* **1937**, *5*, 712–716.
- (2) Rard, J. A.; Rand, M. H.; Anderegg, G.; Wanner, H. Chemical Thermodynamics. In *Chemical Thermodynamics of Technetium*, Sandino, M. C. A.; Östholms, E., Eds.; OECD Nuclear Energy Agency: Issy-les-Moulineaux, France, 1999; Vol. 3.
- (3) Browne, E.; Tuli, J. K. Nuclear Data Sheets for A = 99. *Nucl. Data Sheets* **2017**, *145*, 25–340.
- (4) Pearce, C. I.; Icenhower, J. P.; Asmussen, R. M.; Tratnyek, P. G.; Rosso, K. M.; Lukens, W. W.; Qafoku, N. P. Technetium Stabilization

in Low-Solubility Sulfide Phases: A Review. *ACS Earth Space Chem.* **2018**, *2*, 532–547.

- (5) Hummel, W.; Anderegg, G.; Puigdomènech, I.; Rao, L.; Tochiyama, O. Chemical Thermodynamics. In *Chemical Thermodynamics of Compounds and Complexes of U, Np, Pu, Am, Tc, Se, Ni and Zr with Selected Organic Ligands*; Mompean, F. J.; Illemassene, M.; Perrone, J., Eds.; OECD Nuclear Energy Agency: Issy-les-Moulineaux, France, 2005; Vol. 9.

- (6) Benbow, S. J.; Rivett, M. O.; Chittenden, N.; Herbert, A. W.; Watson, S.; Williams, S. J.; Norris, S. Potential Migration of Buoyant LNAPL from Intermediate Level Waste (ILW) Emplaced in a Geological Disposal Facility (GDF) for UK Radioactive Waste. *J. Contam. Hydrol.* **2014**, *167*, 1–22.

- (7) Maset, E. R.; Sidhu, S. H.; Fisher, A.; Heydon, A.; Worsfold, P. J.; Cartwright, A. J.; Keith-Roach, M. J. Effect of Organic Co-Contaminants on Technetium and Rhenium Speciation and Solubility under Reducing Conditions. *Environ. Sci. Technol.* **2006**, *40*, 5472–5477.

- (8) Reinoso-Maset, E.; Worsfold, P. J.; Keith-Roach, M. J. The Effect of EDTA, NTA and Picolinic Acid on Th(IV) Mobility in a Ternary System with Natural Sand. *Environ. Pollut.* **2012**, *162*, 399–405.

- (9) Wall, N. A.; Karunathilake, N.; Dong, W. Interactions of Tc(IV) with Citrate in NaCl Media. *Radiochim. Acta* **2013**, *101*, 111–116.

- (10) Akram, N.; Bourbon, X. In *Analyse Critique de Données Thermodynamiques: Pouvoir Complexant de l'EDTA, Du NTA, Du Citrate et de l'oxalate Vis à Vis de Cations Métalliques*, ANDRA report C RP O. GES, 1995.

- (11) Gorski, B.; Koch, H. Zur chemie des technetium in wäßriger lösung—I: Über den zustand des vierwertigen technetium in wäßriger lösung. *J. Inorg. Nucl. Chem.* **1969**, *31*, 3565–3571.

- (12) Gorski, B.; Koch, H. Über die komplexbildung von technetium mit chelatbildenden liganden—II. *J. Inorg. Nucl. Chem.* **1970**, *32*, 3831–3836.

- (13) Boggs, M. A.; Islam, M.; Dong, W.; Wall, N. A. Complexation of Tc(IV) with EDTA at Varying Ionic Strength of NaCl. *Radiochim. Acta* **2013**, *101*, 13–18.

- (14) Friend, M. T.; Lledo, C. E.; Lecrivain, L. M.; Wall, D. E.; Wall, N. A. Thermodynamic Parameters for the Complexation of Technetium(IV) with EDTA. *Radiochim. Acta* **2018**, *106*, 963–970.

- (15) Xia, Y.; Hess, N. J.; Felmy, A. R. Stability Constants of Technetium(IV) Oxalate Complexes as a Function of Ionic Strength. *Radiochim. Acta* **2006**, *94*, 137–141.

- (16) Grenthe, I.; Gaona, X.; Plyasunov, A. V.; Rao, L.; Runde, W. H.; Grambow, B.; Konings, R. J. M.; Smith, A. L.; Moore, E. E. Chemical Thermodynamics. In *Second Update on the Chemical Thermodynamics of Uranium, Neptunium, Plutonium, Americium and Technetium*; Ragoussi, M.-E.; Martinez, J. S.; Costa, D., Eds.; OECD Nuclear Energy Agency: Boulogne-Billancourt, France, 2020; Vol. 14.

- (17) Giffaut, E.; Grivé, M.; Blanc, P.; Vieillard, P.; Colàs, E.; Gailhanou, H.; Gaboreau, S.; Marty, N.; Madé, B.; Duro, L. Andra Thermodynamic Database for Performance Assessment: ThermoChimie. *Appl. Geochem.* **2014**, *49*, 225–236.

- (18) Richard, L.; Sabater, C.; Gaona, X.; Grivé, M.; Duro, L. *Contribution to Nancy-Université: NOM Effect on the Mobilization of Radionuclides*, Project ANDRA-TDB6-Task6; Amphos 21, 2010.

- (19) Grivé, M.; Duro, L.; Colàs, E.; Giffaut, E. Thermodynamic Data Selection Applied to Radionuclides and Chemotoxic Elements: An Overview of the ThermoChimie-TDB. *Appl. Geochem.* **2015**, *55*, 85–94.

- (20) Omoto, T.; Wall, N. A. Stability Constant Determinations for Technetium (IV) Complexation with Selected Amino Carboxylate Ligands in High Nitrate Solutions. *Radiochim. Acta* **2017**, *105*, 621–627.

- (21) Omoto, T.; Wall, N. A. Evaluation of Vanadium(IV) as a Non-Radioactive Surrogate for Technetium(IV) by Comparison of Stability Constants for Polyamino Polycarboxylate Ligand Complexation. *J. Solution Chem.* **2017**, *46*, 1981–1994.

- (22) Gaona, X.; Fellhauer, D.; Altmaier, M. Thermodynamic Description of Np(VI) Solubility, Hydrolysis, and Redox Behavior

in Dilute to Concentrated Alkaline NaCl Solutions. *Pure Appl. Chem.* **2013**, *85*, 2027–2049.

(23) Yalcintas, E. *Redox, Solubility and Sorption Chemistry of Technetium in Dilute to Concentrated Saline Systems*; Karlsruher Institut für Technologie: Karlsruhe, Germany, 2015.

(24) Altmaier, M.; Metz, V.; Neck, V.; Müller, R.; Fanghänel, T. Solid-Liquid Equilibria of $\text{Mg}(\text{OH})_2(\text{cr})$ and $\text{Mg}_3(\text{OH})_4\text{Cl}\cdot 4\text{H}_2\text{O}(\text{cr})$ in the System Mg-Na-H-OH-Cl- H_2O at 25 °C. *Geochim. Cosmochim. Acta* **2003**, *67*, 3595–3601.

(25) DiBlasi, N. A.; Tasi, A. G.; Gaona, X.; Fellhauer, D.; Dardenne, K.; Rothe, J.; Reed, D. T.; Hixon, A. E.; Altmaier, M. Impact of Ca(II) on the Aqueous Speciation, Redox Behavior, and Environmental Mobility of Pu(IV) in the Presence of EDTA. *Sci. Total Environ.* **2021**, *783*, No. 146993.

(26) DiBlasi, N. A.; Tasi, A. G.; Trumm, M.; Schnurr, A.; Gaona, X.; Fellhauer, D.; Dardenne, K.; Rothe, J.; Reed, D. T.; Hixon, A. E.; Altmaier, M. Pu(III) and Cm(III) in the Presence of EDTA: Aqueous Speciation, Redox Behavior, and the Impact of Ca(II). *RSC Adv.* **2022**, *12*, 9478–9493.

(27) Zimina, A.; Dardenne, K.; Denecke, M. A.; Doronkin, D. E.; Huttel, E.; Lichtenberg, H.; Mangold, S.; Pruessmann, T.; Rothe, J.; Spangenberg, T.; Steininger, R.; Vitova, T.; Geckeis, H.; Grunwaldt, J.-D. CAT-ACT—A New Highly Versatile x-Ray Spectroscopy Beamline for Catalysis and Radionuclide Science at the KIT Synchrotron Light Facility ANKA. *Rev. Sci. Instrum.* **2017**, *88*, No. 113113.

(28) Ravel, B.; Newville, M. ATHENA, ARTEMIS, HEPHAESTUS: Data Analysis for X-Ray Absorption Spectroscopy Using IFEFFIT. *J. Synchrotron Radiat.* **2005**, *12*, 537–541.

(29) Rodriguez, E. E.; Poineau, F.; Llobet, A.; Sattelberger, A. P.; Bhattacharjee, J.; Waghmare, U. V.; Hartmann, T.; Cheetham, A. K. Structural Studies of TcO_2 by Neutron Powder Diffraction and First-Principles Calculations. *J. Am. Chem. Soc.* **2007**, *129*, 10244–10248.

(30) Ciavatta, L. The Specific Interaction Theory in Evaluating Ionic Equilibria. *Ann. Chim.* **1980**, *70*, 551.

(31) Hummel, W. *Ionic Strength Corrections and Estimation of SIT Ion Interaction Coefficients*, PSI Technical Report, Paul Scherrer Institut: Villigen, Switzerland, 2009.

(32) Puigdomènech, I. In *Windows Software for the Graphical Presentation of Chemical Speciation*, Abstracts of Papers: 219th ACS National Meeting, American Chemical Society: Washington, DC, 2000.

(33) Puigdomènech, I.; Colàs, E.; Grivé, M.; Campos, I.; García, D. A Tool to Draw Chemical Equilibrium Diagrams Using SIT: Applications to Geochemical Systems and Radionuclide Solubility. *MRS Online Proc. Libr.* **2014**, *1665*, 111–116.

(34) Oliveira, A. F.; Kuc, A.; Heine, T.; Abram, U.; Scheinost, A. C. Shedding Light on the Enigmatic $\text{TcO}_2\cdot x\text{H}_2\text{O}$ Structure with Density Functional Theory and EXAFS Spectroscopy. *Chem. - Eur. J.* **2022**, *28*, No. e202202235.

(35) Yalçintaş, E.; Gaona, X.; Altmaier, M.; Dardenne, K.; Polly, R.; Geckeis, H. Thermodynamic Description of Tc(IV) Solubility and Hydrolysis in Dilute to Concentrated NaCl, MgCl_2 and CaCl_2 Solutions. *Dalton Trans.* **2016**, *45*, 8916–8936.

(36) Dardenne, K.; Duckworth, S.; Gaona, X.; Polly, R.; Schimmelpfennig, B.; Pruessmann, T.; Rothe, J.; Altmaier, M.; Geckeis, H. A Combined Study of Tc Redox Speciation in Complex Aqueous Systems: Wet-Chemistry, Tc K-/L3-Edge X-Ray Absorption Fine Structure, and Ab Initio Calculations. *Inorg. Chem.* **2021**, *60*, 12285–12298.

(37) Rand, M.; Fuger, J.; Grenthe, I.; Neck, V.; Rai, D. Chemical Thermodynamics. In *Chemical Thermodynamics of Thorium*, Mompean, F. J.; Perrone, J.; Illemassene, M., Eds.; OECD Nuclear Energy Agency: Issy-les-Moulineaux, France, 2008; Vol. 11.

(38) Tasi, A.; Gaona, X.; Rabung, T.; Fellhauer, D.; Rothe, J.; Dardenne, K.; Lützenkirchen, J.; Grivé, M.; Colàs, E.; Bruno, J.; Källstrom, K.; Altmaier, M.; Geckeis, H. Plutonium Retention in the Isosaccharinate—Cement System. *Appl. Geochem.* **2021**, *126*, No. 104862.

(39) Gaona, X.; Montoya, V.; Colàs, E.; Grivé, M.; Duro, L. Review of the Complexation of Tetravalent Actinides by ISA and Gluconate under Alkaline to Hyperalkaline Conditions. *J. Contam. Hydrol.* **2008**, *102*, 217–227.